Plant Diversity 44 (2022) 377–388

Contents lists available at ScienceDirect

Plant Diversity

journal homepage: http://www.keaipublishing.com/en/journals/plant-diversity/
http://journal.kib.ac.cn

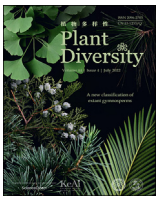

Research paper

Plastid genome evolution of a monophyletic group in the subtribe Lauriineae (Laureae, Lauraceae)

Chao Liu [a], Huan-Huan Chen [a], Li-Zhou Tang [a], Phyo Kay Khine [c], Li-Hong Han [a, **], Yu Song [b, *], Yun-Hong Tan [c, d, ***]

[a] College of Biological Resource and Food Engineering, Yunnan Engineering Research Center of Fruit Wine, Qujing Normal University, Qujing, Yunnan, 655011, China
[b] Key Laboratory of Ecology of Rare and Endangered Species and Environmental Protection (Ministry of Education), Guangxi Key Laboratory of Landscape Resources Conservation and Sustainable Utilization in Lijiang River Basin, Guangxi Normal University, Guilin, Guangxi, 541004, China
[c] Center for Integrative Conservation, Xishuangbanna Tropical Botanical Garden, Chinese Academy of Sciences, Mengla, Yunnan, 666303, China
[d] Southeast Asia Biodiversity Research Institute, Chinese Academy of Sciences, Yezin, Nay Pyi Taw, 05282, Myanmar

ARTICLE INFO

Article history:
Received 20 May 2021
Received in revised form
28 November 2021
Accepted 29 November 2021
Available online 14 December 2021

Keywords:
Litsea
Phylogenetic analysis
Divergent hotspots
Gene evolution

ABSTRACT

Litsea, a non-monophyletic group of the tribe Laureae (Lauraceae), plays important roles in the tropical and subtropical forests of Asia, Australia, Central and North America, and the islands of the Pacific. However, intergeneric relationships between *Litsea* and *Laurus*, *Lindera*, *Parasassafras* and *Sinosassafras* of the tribe Laureae remain unresolved. In this study, we present phylogenetic analyses of seven newly sequenced *Litsea* plastomes, together with 47 Laureae plastomes obtained from public databases, representing six genera of the Laureae. Our results highlight two highly supported monophyletic groups of *Litsea* taxa. One is composed of 16 *Litsea* taxa and two *Lindera* taxa. The 18 plastomes of these taxa were further compared for their gene structure, codon usage, contraction and expansion of inverted repeats, sequence repeats, divergence hotspots, and gene evolution. The complete plastome size of newly sequenced taxa varied between 152,377 bp (*Litsea auriculata*) and 154,117 bp (*Litsea pierrei*). Seven of the 16 *Litsea* plastomes have a pair of insertions in the IRa (*trnL-trnH*) and IRb (*ycf2*) regions. The 18 plastomes of *Litsea* and *Lindera* taxa exhibit similar gene features, codon usage, oligonucleotide repeats, and inverted repeat dynamics. The codons with the highest frequency among these taxa favored A/T endings and each of these plastomes had nine divergence hotspots, which are located in the same regions. We also identified six protein coding genes (*accD*, *ndhJ*, *rbcL*, *rpoC2*, *ycf1* and *ycf2*) under positive selection in *Litsea*; these genes may play important roles in adaptation of *Litsea* species to various environments.

1. Introduction

The genus *Litsea* Lamarck in the family Lauraceae, which is regarded as the 'core Laureae' or *Litsea* complex, is one of the most diverse genera of evergreen and rare deciduous trees or shrubs (Kamle et al., 2019). *Litsea* comprises approximately 400 known species and is distributed in the tropical and subtropical forests of Asia, Australia, Central and North America, and the islands of the Pacific (Fijridiyanto and Murakami, 2009a). *Litsea* species are economically important as a source of medicine, spices, and perfumes (Wang et al., 2016), and serve as food for Muga silk worms (*Antheraea assama*) (Yadav and Goswami, 1990). In addition, *Litsea* grow in mixed wood forest or forest edge, some of which used as garden trees, which play a critical role in ecoregulation. The genus *Litsea* was divided by Bentham (1880) into four sections: sect. *Conodaphne* (Bl.) Benth. et Hook. f., sect. *Cylicodaphne* (Nees) Hook. f., sect. *Litsea*, and sect. *Tomingodaphne* (Bl.) Hook. f. However, more recent studies have found that several *Litsea* species are nested within different sections. For example, some species of section

* Corresponding author.
** Corresponding author.
*** Corresponding author. Center for Integrative Conservation, Xishuangbanna Tropical Botanical Garden, Chinese Academy of Sciences, Mengla, Yunnan, 666303, China.
E-mail addresses: hanlihong9527@126.com (L.-H. Han), songyu@xtbg.ac.cn (Y. Song), tyh@xtbg.org.cn (Y.-H. Tan).
Peer review under responsibility of Editorial Office of Plant Diversity.

https://doi.org/10.1016/j.pld.2021.11.009

Conodaphne are more closely related to *Lindera* than to other *Litsea* sections (Fijridiyanto and Murakami, 2009b). In addition, *Litsea* and *Lindera* have been shown to be anatomically and morphologically polyphyletic, and closely related to *Laurus*, *Dodecadenia* Nees, *Iteadaphne* Blume, *Parasassafras* D.G. Long and *Sinosassafras* H.W. Li (Li and Christophel, 2000; Li et al., 2008; Chanderbali et al., 2001; Song et al., 2020; Zhang et al., 2021). Delimiting the genera of the *Litsea* complex and understanding their phylogenetic relationships remains a major challenge.

Plastid and nuclear DNA barcoding markers have been used to provide effective molecular information for identification and comparison of closely related species or genera (Li et al., 2004; Fijridiyanto and Murakami, 2009b; Song et al., 2016, 2017, 2020). Using the chloroplast gene *matK* and nuclear ribosomal DNA ITS sequences, Li et al. (2004) conducted a phylogenetic analysis of the 'core' Laureae based on Chinese materials, and found that *Litsea* clustered with *Laurus*, *Parasassafras*, and *Lindera* in a polytomy. The phylogenetic analyses of *rpb2* showed *Litsea* and *Lindera* were polyphyletic (Fijridiyanto and Murakami, 2009b). Although different phylogenetic relationships among core Laureae have been investigated using chloroplast markers combined with nuclear ribosomal genes in previous studies (Li et al., 2004, 2008; Fijridiyanto and Murakami, 2009b), both the generic delimitation and species relationships within the genus *Litsea* still remain ambiguous. At present, high-throughput sequencing approaches might provide a better understanding of the relationships among species and genera in Lauraceae.

In recent years, complete plastid genomes have been widely used to study plant taxonomy and evolution in the family Lauraceae (Song et al., 2016, 2017, 2020; Tian et al., 2019; Xiao et al., 2020). Plastomes are ideal molecular markers for species identification and phylogenetic analysis because they are haploid, maternally inherited, and have a highly conserved structure, low mutation rates and a slow evolutionary rate (Du et al., 2020; Henriquez et al., 2020; Zheng et al., 2020). Comparative analysis of plastome structure and genetic diversity can help delimit genera and clarify phylogenetic relationships within the Lauraceae family. Currently, the plastome sequences of over ten *Litsea* species are available (Hinsinger and Strijk, 2017; Hinsinger and Strijk, 2017; Jo et al., 2019; Liu et al., 2020; Xiao et al., 2020).

Previous studies have used Lauraceae plastome sequences for phylogenetic analysis of Lauraceae (see Song et al., 2020, which reconstructed six monophyletic groups as the supergeneric classification of the Lauraceae). The tribe Laureae has been divided into at least five subgroups and *Litsea* taxa grouped into two subclades (Song et al., 2020). The first monophyletic group is composed of trinerved *Lindera* species and *Iteadaphne caudata* (Tian et al., 2019). In this study, we sequenced seven *Litsea* plastomes and compared the plastome structures of *Litsea* and *Lindera* taxa to identify the second monophyletic group in the Subtribe Lauriinae. This monophyletic group is composed of *Litsea* species and *Lindera obtusiloba*. We also identified divergence hotspot regions within the newly sequenced plastomes and detected protein coding sequences under positive selection.

2. Materials and methods

2.1. Sampling, DNA extraction and sequencing

Fresh young leaves of seven taxa (*Litsea auriculata* S.S. Chien & W.C. Cheng, *Litsea dilleniifolia* P.Y. Pai & P.H. Huang, *Litsea lancilimba* Merr., *Litsea liyuyingi* H. Liu, *Litsea pierrei* Lecomte, *L. pierrei* var. *szemois* Liou, *Litsea cubeba* var. *formosana* (Nakai) Y.C. Yang & P.H. Huang) were obtained and dried in silica gel. The harvested tissues were deposited at the Biodiversity Research Group of Xishuangbanna Tropical Botanical Garden, Chinese Academy of Sciences (Table 1). Total genomic DNA was extracted from the leaves following the cetyltrimethylammonium bromide (CTAB) protocol (Doyle and Dickson, 1987). Long-range PCR was performed following Zhang et al. (2016), with their 15 universal primer pairs for next-generation sequencing. A total of 6 μg of DNA was further fragmented into small pieces by Covaris S220, and paired-end libraries were constructed following the manufacturer's instructions (Illumina, San Diego, CA, USA). Sequencing was performed on an Illumina Genome Analyser Hiseq 2000 at Beijing Genomics Institute (Shenzhen, China).

2.2. Plastome assembly and annotation

Raw reads were filtered to remove low-quality reads, and de novo assembly of circular plastomes was carried out using GetOrganelle software (Jin et al., 2020). Plastomes were adjusted and annotated using Geneious v.8.1.3 (Kearse et al., 2012) and GeSeq (https://chlorobox.mpimp-golm.mpg.de/geseq.html) against the referenced plastid genome sequence of *Litsea cubeba* (Accession No. MT431385). Manual adjustment was carried out with published plastomes as a reference to confirm the boundaries between large single copy (LSC), small single copy (SSC), and inverted repeat (IR) regions. The precise locations of start and stop codons and the exons and introns of genes were carefully assigned manually. The output GenBank files were inspected and edited manually, and circular plastome maps were drawn using OGDRAW v.1.3.1 (Greiner et al., 2019).

2.3. Phylogenetic analysis

To determine phylogenetic relationships of the "core Laureae" species, we compared the complete plastomes of 54 taxa of Lauraceae species available at NCBI and LCGDB (http://lcgdb.wordpress.com) (Song et al., 2020; Xiao et al., 2020) (Table S1), including two taxa each from *Iteadaphne* and *Parasassafras*, two from *Laurus*, 21 from *Litsea*, 27 from *Lindera*. We used two taxa from *Cinnamomum* Schaeff. as outgroups.

Coding sequences (CDS) were also extracted and used for phylogenetic reconstruction. Multiple sequence alignments were initially done using MAFFT v.7.450 (Katoh et al., 2019) and manually edited where necessary with BioEdit v.7.0.9. Bayesian inference (BI) was performed using BEAST v.2.6.3 (Bouckaert et al., 2014) and the best substitution model ('TVM + F') was tested by AIC in IQ-TREE v.2.1.1 (Minh et al., 2020). Maximum likelihood (ML) analysis was performed using IQ-TREE (Minh et al., 2020) with the GTR + F + R2 model of nucleotide substitution and 1000 bootstrap replicates.

2.4. Sequence analysis

To assess evolutionary changes in the newly sequenced *Litsea* plastomes, we characterized plastome structure, including contractions and expansions of IR regions, and analyzed codon usage, repeats, and SSRs. The relative synonymous codon usage (RSCU) was obtained using CodonW v.1.4.2 (http://codonw.sourceforge.net/) with protein-coding genes >200 bp in size. GC content of the complete plastomes and the coding sequences were analysed using Mega X (Kumar et al., 2018). Long repetitive sequences were identified using REPuter web-service program (https://bibiserv.Cebitec.uni-bielefeld.de/reputer) (Kurtz et al., 2001). Forward (F), reverse (R), complementary (C), and palindromic (P) repeats were analysed with a minimum repeat size of 30 bp, a sequence identity of 90% and a Hamming distance of 3. Simple sequence repeats (SSRs) were detected using the MISA-web service (https://webblast.ipk-gatersleben.de/misa/) (Beier et al., 2017). SSR

Table 1
Summary of plastomes features of seven *Litsea* taxa.

Genome feature		*Litsea auriculata*	*Litsea dilleniifolia*	*Litsea lancilimba*	*Litsea liyuyingi*	*Litsea pierrei*	*Litsea pierrei* var. *szemois*	*Litsea cubeba* var. *formosana*
Voucher		SY36036	M5501	SY36053	SY35772	Y1022	SY36665	SY36958
Accessions		LAU00101	LAU00102	LAU00103	LAU00104	LAU00105	LAU00106	LAU00107
Length (bp)	Genome	152,377	153,555	154,113	152,824	154,117	154,035	154,093
	LSC	93,533	93,135	93,754	93,810	93,738	93,124	93,676
	SSC	18,814	18,884	18,767	18,834	18,799	18,333	18,933
	IR	20,015	20,768	20,796	20,090	20,790	21,289	20,742
GC content %	Genome	39.15	39.24	39.18	39.18	39.22	39.22	39.17
	LSC	37.93	38.04	37.97	37.96	38.01	38.05	37.97
	SSC	33.94	33.99	33.97	34.06	34.06	34.12	33.87
	IR	44.45	44.32	44.27	44.43	44.29	43.96	44.70
Gene number (unique)	Genome	126 (113)	126 (113)	126 (113)	126 (113)	126 (113)	126 (113)	126 (113)
	CDS	82 (79)	82 (79)	82 (79)	82 (79)	82 (79)	82 (79)	82 (79)
	rRNA	8 (4)	8 (4)	8 (4)	8 (4)	8 (4)	8 (4)	8 (4)
	tRNA	36 (30)	36 (30)	36 (30)	36 (30)	36 (30)	36 (30)	36 (30)

analysis was employed with a minimum threshold of ten nucleotides for mononucleotides, five for dinucleotides, four for trinucleotides, and three for tetranucleotides, pentanucleotides, and hexanucleotides. The nucleotide diversity (Pi) value was calculated through alignment of the complete plastome sequences of different species using DnaSP v.6.0 (Rozas et al., 2017), with the window length set to 600 bp and a 200-bp step size. Values were plotted in the R program. Gene organization maps were drawn in TBtools v.1.064 (Chen et al., 2020). Expansion and contraction of IRs was analysed using the IRscope online program (https://irscope.shinyapps.io/irapp/). To evaluate variation in evolutionary rates of plastomes, we examined 82 protein-coding regions in 18 taxa belonging to one monophyletic group of sect. *Litsea* (16 *Litsea* species and 2 *Lindera* species). The site model was performed to test for potential positive selection using the CODEML algorithm in PAMLX v.1.3.1 under a phylogenetic framework (Xu and Yang, 2013). The ratios of non-synonymous (dN) to synonymous (dS) substitutions (dN/dS) in protein-coding genes were estimated. Two likelihood ratio tests (LRT) of M1 (nearly neutral) vs. M2 (positive selection) and M7 (beta) vs. M8 (beta and ω) were used to check for sites with evidence of positive selection. The posterior probabilities for evolutionary potential under selection were calculated using the Bayes empirical Bayes (BEB) method. The species *Litsea cubeba* (MT431385) was used as a reference.

3. Results

3.1. Characteristics of the seven newly obtained Litsea plastomes

In this study, we sequenced seven *Litsea* plastomes. Plastome sizes ranged from 152,377 bp (*L. auriculata*) to 154,117 bp (*L. pierrei*) (Fig. 1). The typical quadripartite structure was found for all seven taxa: a pair of IRs (IRa and IRb) of 20,015–21,289 bp separated by one LSC region of 92,643–94,311 bp and one SSC region of 18,333–18,814 bp. The plastomes of two species (*L. dilleniifolia* and *L. pierrei* var. *szemois*) lost a 660-bp fragment between two poly-A/T sequences. GC content was similar in all seven plastomes (39.15%–39.24%). GC content (43.96%–44.70%) in the IR regions was higher than that in the LSC (37.93%–38.05%) and SSC regions (33.87%–34.12%). GC content in protein-coding genes was 39.36%. A total of 113 single copy genes were detected in each plastome, including four rRNA genes, 30 tRNA genes, and 79 protein-coding genes. In addition, 13 duplicated genes were located in the IR regions (Tables 1 and S2). Among the protein coding genes, nine genes (*atpF*, *ndhA*, *ndhB*, *petB*, *petD*, *rpl2*, *rpl16*, *rpoC1* and *rps16*) displayed one intron each; three genes (*clpP*, *rps12* and *ycf3*) contained two introns each.

3.2. Phylogenomic analysis

To understand the evolutionary relationships between *Litsea* taxa, we reconstructed a Laureae phylogenetic tree using the plastomes of 54 Lauraceae taxa, including our seven newly sequenced *Litsea* plastomes and plastomes of 14 additional *Litsea* taxa. The phylogenetic trees inferred from ML and BI analyses were topologically congruent, and the phylogenetic topology of trees based on complete plastomes and coding sequences was the same, with similar values of branch support (Figs. 2 and S1). Thus, here we only show the Bayesian tree based on complete plastomes. The 54 Lauraceae taxa were divided into at least four clades with strong support, excluding the two *Cinnamomum* species, which served as outgroups. Clade I included two *Laurus*, seven *Lindera*, and five *Litsea* taxa; Clade II included four *Lindera* species; Clade III included two *Lindera*, and 16 *Litsea* taxa; Clade IV included one *Iteadaphne*, one *Parasassafras*, and 14 *Lindera* taxa. The 21 *Litsea* taxa were clustered into two clades (Clade I and Clade III), and the seven newly obtained *Litsea* taxa were located in the same sub-clade with an additional nine *Litsea* and two *Lindera obtusiloba* taxa. Clade III was split into four major subclades: clade IIIa (*Litsea cubeba* var. *formosana*, *L. mollis*, *L. cubeba*, *L. panamonja*, *Lindera obtusiloba* var. *heterophylla*, *L. obtusiloba*), clade IIIb (*L. auriculata*, *L. coreana*), clade IIIc (*L. elongata*, *L. japonica*, *L. garrettii*, *L. monopetala*), and clade IIId (*L. dilleniifolia*, *L. szemaois*, *L. pierrei*, *L. pierrei* var. *szemois*, *L. liyuyingi*, *L. lancilimba*).

3.3. Codon usage and amino acid frequency

In clade III, each of the 18 plastomes possessed 82 protein-coding genes, which were encoded by 64 different codons, including three stop codons (TAA, TAG and TGA, Fig. 3). RSCU analyses revealed that codons that ended with A/T at the third base had RSCU >1 and encoded the highest number of amino acids. The codons that ended with C/G at the third base had RSCU <1 and encoded the lowest number of amino acids (Fig. 3). Most of the high frequency codons and 29 out of 31 optimal codons ended with A/T. Among the 64 codons, AGC-encoded serine and CGC-encoded arginine had the lowest RSCU values (0.35), and AGA-encoded arginine had the highest RSCU values (1.82). The ATG codon, which encodes formyl-methionine as a start codon, was the most common start codon in this study. However, alternate codons were also found as start codons, such as GTG (in *cemA* and *rps19*), TTG (in *ndhD* and *rpl2*), CTG (in *psbL*) and ACT (in *rps12*), which has also been reported in other plant species (Henriquez et al., 2020; Zheng et al., 2020). Moreover, the analysis of amino acid frequencies revealed that leucine (Leu, 10%) and cysteine (Cys, 1%) were the

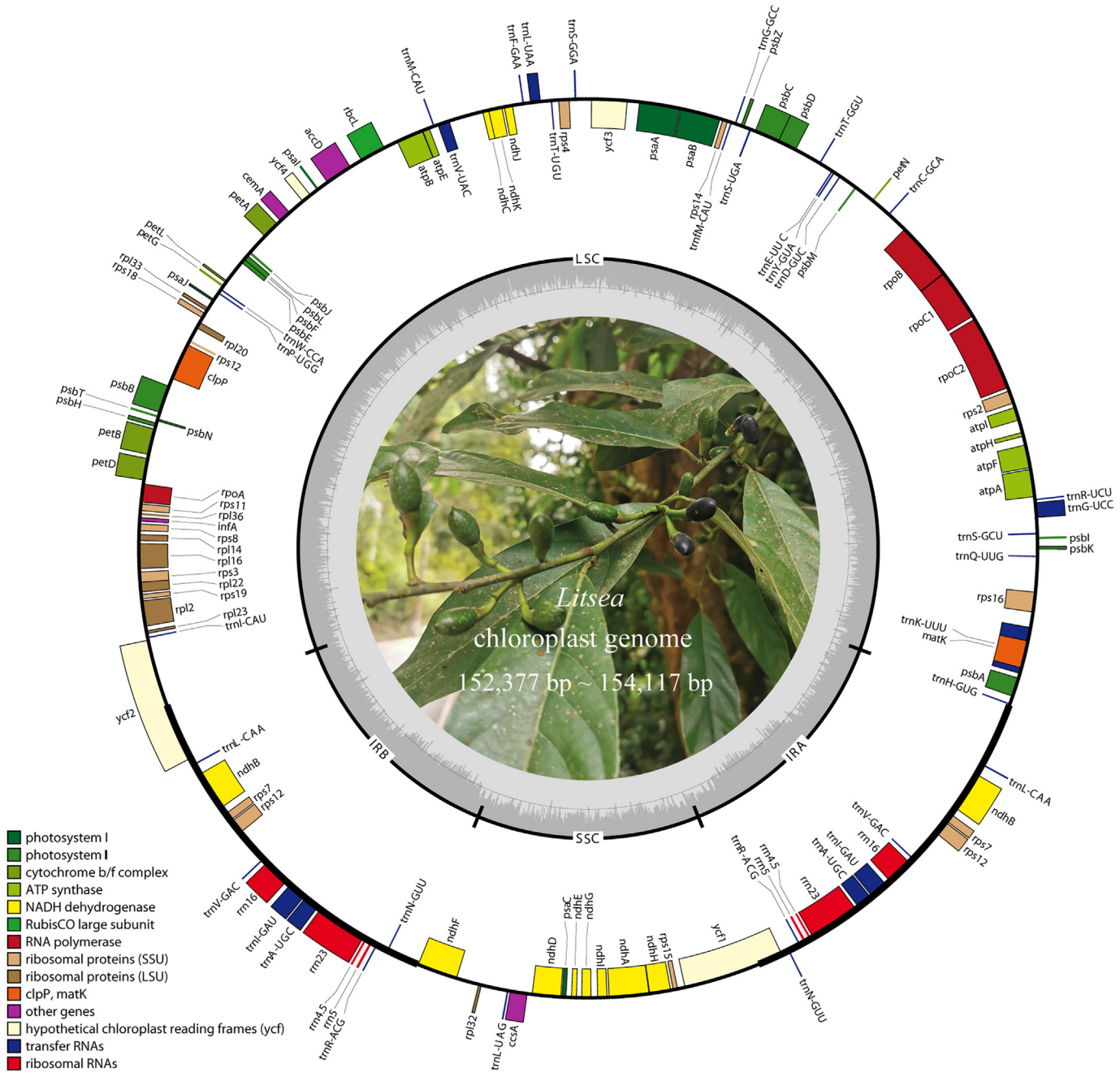

Fig. 1. Gene map of the *Litsea* plastomes. *Litsea garrettii* is shown.

most and the least frequent amino acids, respectively (Fig. S2). In general, codon usage and amino acid frequency were similar across the 18 taxa.

3.4. Contraction and expansion of inverted repeats

Contractions and expansions of inverted repeats at the junctions of LSC/IRb, IRb/SSC, SSC/IRa, and IRa/LSC revealed that the plastomes of the 18 taxa in clade III are highly similar. *L. pierrei* var. *szemois* has the longest IR region (21,289 bp), whereas *L. auriculata* has the shortest (20,015 bp), with a difference of 1274 bp.Thus, the lengths of the IR regions of the 18 taxa are very different. The *ycf2* gene spans the LSC/IRb boundary, and partially extends into the IRb region that ranges from 3159 bp to 3863 bp in length. The *ndhF* gene spans the IRb/SSC boundary, and the portion located in the IRb region ranges from five to 12 bp in length. The *ycf1* gene spans the junction of the SSC and IRa regions, and the length of the *ycf1* gene extends into the IRa region, ranging from 5456 bp to 5588 bp. Finally, the *trnH* gene is completely located in the LSC region at the junction of the IRa/LSC, and its distance from the boundary line is between 21 bp to 27 bp. Overall, the 18 taxa show similar characteristics at the IR/SC boundary regions. The LSC and SSC regions are more divergent between species than the two IR regions, and the intergenic regions exhibit higher divergence than the coding regions. In the alignment analysis, seven regions (*trnG-trnR*, *psbM-trnD*, *ycf3-trnS*, *ndhF-rp132-trnL* and *ycf1*) with low identity were detected (Fig. S3). The plastomes of seven *Litsea* species (*L. dilleniifolia*, *L. elongata*, *L. garrettii*, *L. lancilimba*, *L. pierrei*,

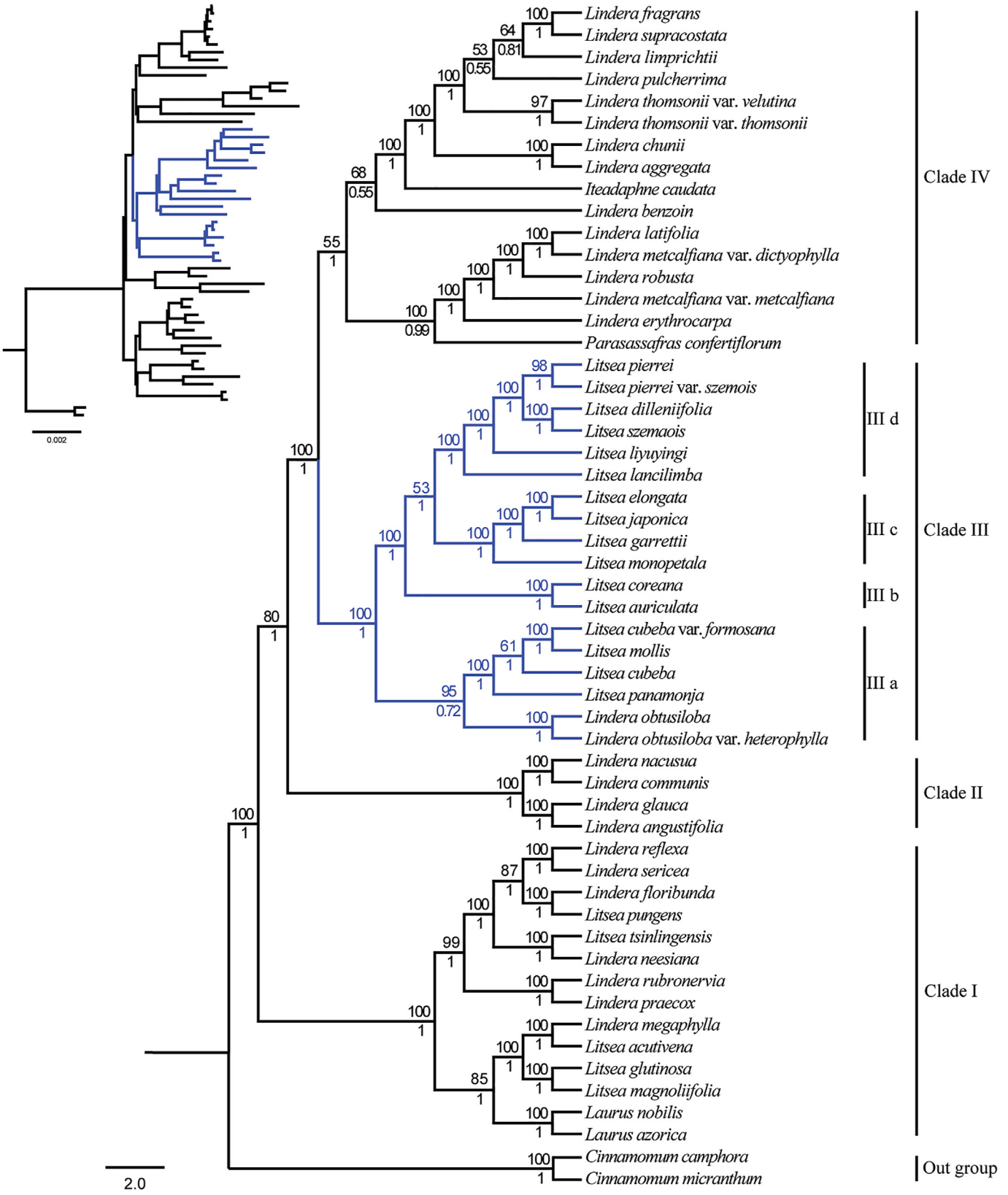

Fig. 2. Bayesian tree of 54 Laureae based on plastome sequence data. Numbers above nodes are bootstrap values. Blue branches represent the 18 taxa analysed in this study.

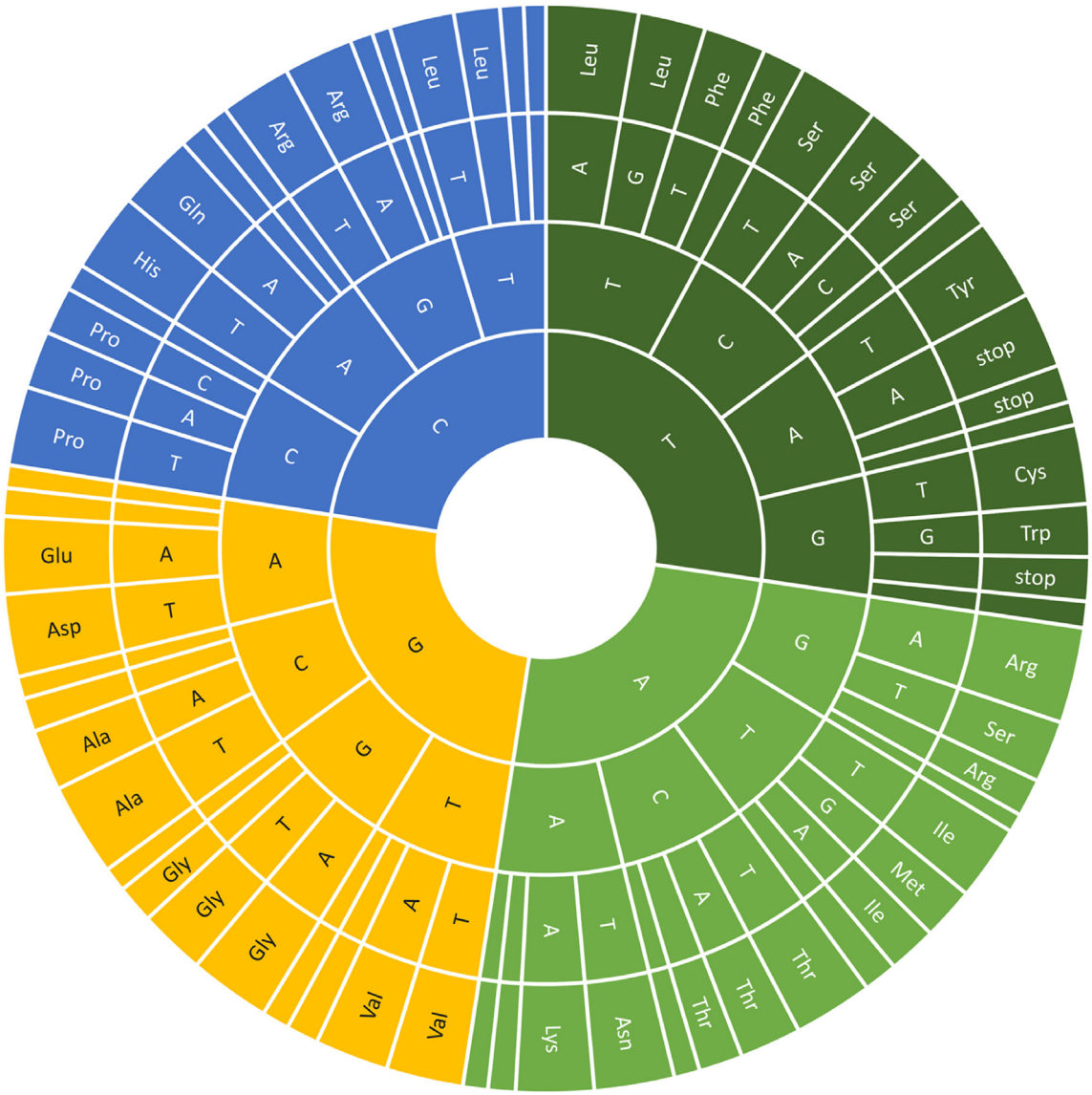

Fig. 3. Codon-anticodon recognition patterns and codon usage in plastomes of the 18 taxa.

L. pierrei var. *szemois*, *L. cubeba* var. *formosana*) have a 678-bp insertion in the IRa (intergenic region) and IRb (*ycf2*) regions, enlarging their genome size (Table 1; Fig. S4). The gene order between the two IR regions is highly conserved in the plastomes of the 18 tax of clade III.

3.5. Repeat analysis

Four types of oligonucleotide repeats — palindromic, reverse, forward, and complement repeats — were detected in the plastomes of the 18 taxa in clade III (Fig. 4). A total of 555 long repeats, consisting of 226 forward repeats and 217 palindromic repeats, were detected (Fig. 4A). The forward, palindromic and reverse repeats were abundant in *L. japonica*, *L. dilleniifolia*, and *L. cubeba* var. *formosana,* respectively. The size of repeats varied among species, but most of the repeat sizes were in the range of 30–34 bp (Fig. 4B). Among the 18 taxa, *L. pierrei* var. *szemois* and *L. garrettii*/*L. monopetala* had the largest (39) and smallest (24) number of repeats. The number of forward repeats varied between nine (*L. garrettii*) and 16 (*L. japonica*), and the number of palindromic repeats varied from 10 (*L. cubeba*, *L. cubeba* var. *formosana*, *L. mollis* and *L. panamonja*) to 16 (*L. dilleniifolia*). The lengths of forward repeats in the 18 species ranged from 30 to 57 bp, and the lengths of palindromic repeats varied from 30 to 60 bp. The number, length and distribution of these sequences varied among the 18 taxa (Fig. 4A).

3.6. SSR analysis

Due to high levels of polymorphism, SSRs are often used as genetic markers to identify closely related species. We compared the distribution and number of SSRs in the plastomes of the 18 taxa in clade III. SSRs ranging from mononucleotide to hexanucleotide repeats were found, but not in all species (Fig. 5A). We identified 1537 SSRs from the 18 plastomes, including 1092 mononucleotide (71.05%), 177 dinucleotide (11.52%), 67 trinucleotide (4.36%), 160 tetranucleotide (10.41%), 21 pentanucleotide (1.37%), and 20 hexanucleotide (1.30%). The first four types of SSR repeats were present in each of the 18 taxa, while the pentanucleotide repeats were absent in *L. pierrei* var. *szemois*, and hexanucleotide repeats were

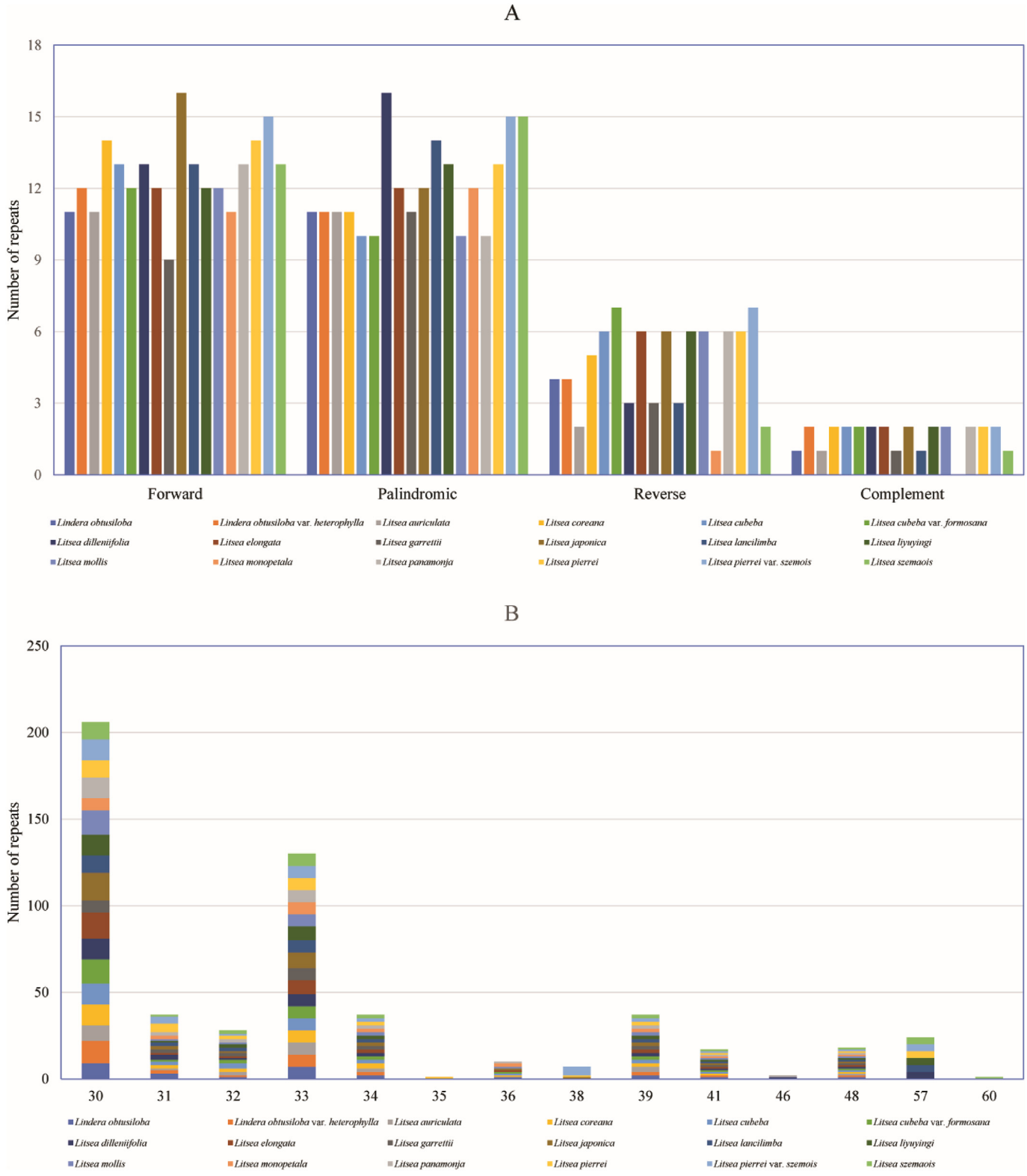

Fig. 4. Number of long repetitive repeats in plastome sequences of the 18 taxa. A. Frequency of repeat type. B. Frequency of repeats >30 bp.

absent in *L. auriculata* and *L. liyuyingi*. The maximum and minimum length of the SSRs was 27 bp (A/T in *L. coreana*), and eight bp (in all 18 taxa), respectively. On average, mononucleotide repeats were the most abundant, accounting for 71.05% of the SSRs, followed by dinucleotide repeats (11.52%) and tetranucleotide repeats (10.41%) (Fig. 5B). *L. monopetala* and *L. mollis* had the most (95) and the fewest SSRs (77), respectively. There were no significant differences in the number of SSRs among the 18 taxa.

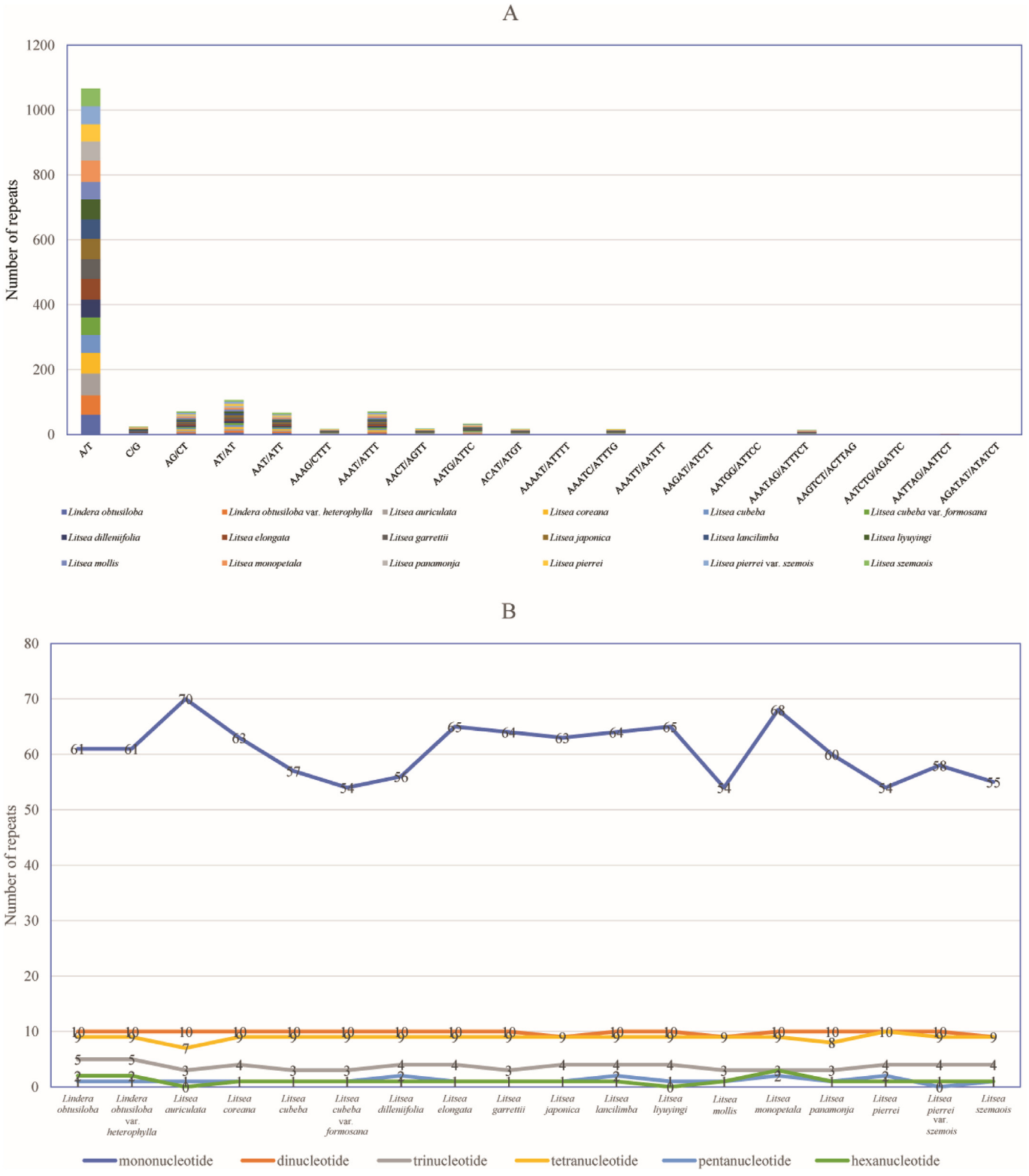

Fig. 5. Number of SSRs in plastome sequences of the 18 taxa. A. Frequency of repeats >30 bp. B. Frequency of repeat type.

3.7. *Divergence hotspots*

Nucleotide diversity (Pi) values were analysed by DnaSP to measure divergence levels within different plastome regions of the 18 taxa in clade III. The alignment size was 156,419 bp, of which 150,516 (about 96.2%) sites were constant, and 2685 (about 1.7%) nucleotide sites were polymorphic. Pi values ranged from 0 to 0.01854, and the average value was 0.00367 (Fig. 6). In the LSC region, Pi values ranged from 0.00019 to 0.01241, with an average of 0.00416, and in the SSC region, they ranged from 0.00277 to

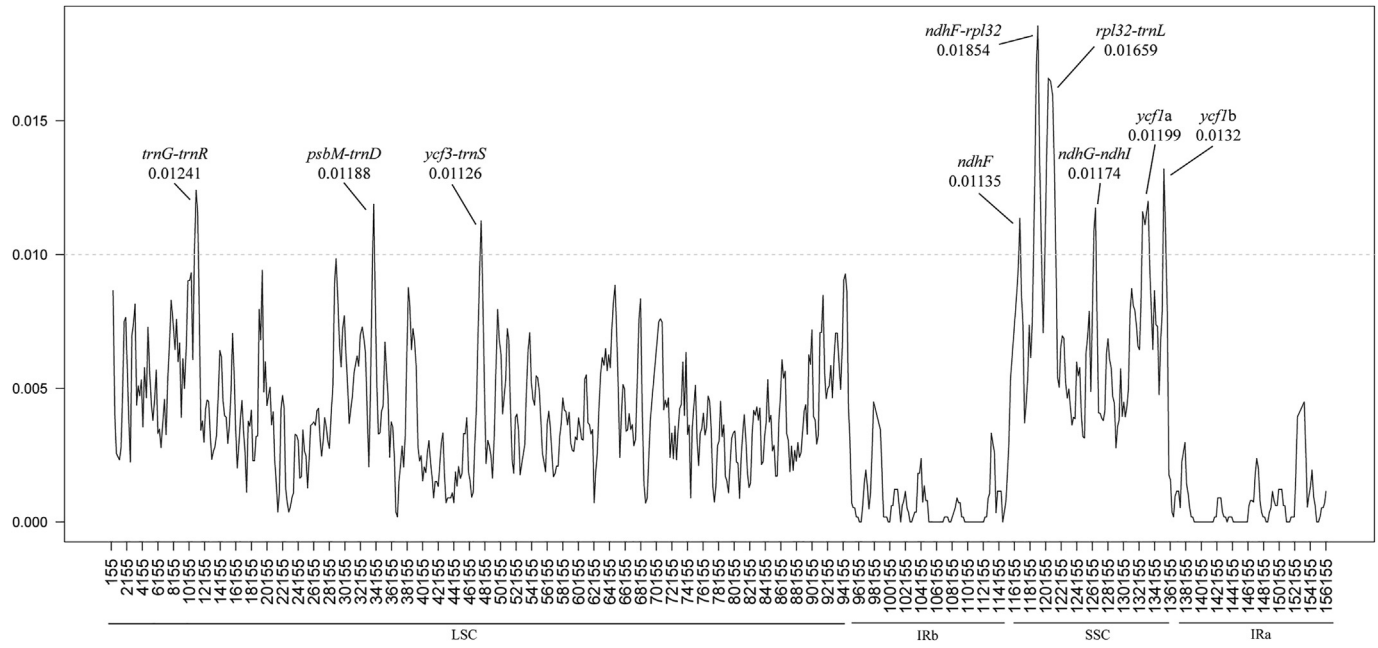

Fig. 6. Nucleotide variability (Pi) values in aligned plastomes from 18 taxa.

0.01854, with an average value of 0.00749; the IR region, in which Pi values ranged from 0 to only 0.00534, had the lowest average value (0.00075) (Fig. 6). Within the nine divergence hotspots, three regions (*trnG-trnR*, *psbM-trnD* and *ycf3-trnS*) were located in the LSC region and six regions (*ndhF*, *ndhF-rpl32*, *rpl32-trnL*, *ndhG-ndhI*, *ycf1*a, and *ycf1*b) were in the SSC region. No variation in the IR regions implies that these regions are more conserved than the SSC and LSC regions. The relatively higher divergence of *ndhF*, *rpl32* and *ycf1* genes than other coding regions has been previously observed in other plastomes (Zheng et al., 2020).

3.8. Selective pressure analysis of protein-coding genes

To test whether the plastid genes of the 18 taxa in clade III had undergone selection, we estimated the rate of dS, dN, and the ratio of dN/dS based on function classification (Fig. 7). The dN/dS ratios were used to estimate the selective pressure in the context of a codon substitution model, with dN/dS < 1, dN/dS = 1, and dN/dS > 1 denoting purifying, neutral, and positive selections, respectively. The dN/dS values were less than 1 for most genes (74 of 79; 93.7%), indicating that purifying selection was acting on these genes. Five genes (*rps16*, *petA*, *ndhC*, *rps3,* and *rpoA*) in the analysed plastomes showed average dN/dS ratios higher than 1, indicating positive selection had been exerted on these genes. A total of 20 protein coding genes obtained feedback results based on BEB analysis (Table S3). Of these, nine genes contained at least one positively selected site with significant posterior probabilities, and *rbcL*, *rpoA*, *rpoB*, *rpoC2*, *ycf1,* and *ycf2* possessed three or more significantly and positively selected sites. Six protein-coding genes (*accD*, *ndhJ*, *rbcL*, *rpoC2*, *ycf1,* and *ycf2*) rejected the null model ($P < 0.01$), corroborating the hypothesis that some amino acid sites in these proteins had been under positive selection. Positive selection of these genes indicates that they are undergoing essential adaptations to their environment despite the weak selection pressures experienced by *Litsea*.

4. Discussion

4.1. Phylogenomic and comparative analysis

The systematics of the “core Lauraceae” group remain in dispute (Tian et al., 2019; Xiao et al., 2020). Previous studies have divided the “core Lauraceae” into two or five major clades based on complete plastome sequences (Zhao et al., 2018; Tian et al., 2019). Furthermore, representatives of the sections of *Litsea* genera have been described as polyphyletic (Li et al., 2008). Here, we used complete plastome sequences of 54 Laureae species to determine the phylogenetic positions of Laureae species. In contrast to previous studies, we found that the “core Lauraceae” can be divided into four clades with strong support. Sixteen of 21 *Litsea* taxa and two *Lindera* taxa clustered in clade III, forming a monophyletic lineage. The genus *Litsea* can be divided into four sections, as proposed by Bentham (1880), with *L. coreana* and *L. monopetala* belonging to section *Conodaphne*; *Litsea glutinosa* belonging to section *Litsea*; *L. auriculata*, *L. cubeba*, *L. cubeba* var. *formosana*, *L. mollis*, *L. pungens*, and *L. tsinlingensis* belonging to section *Tomingodaphne*; and the other eleven *Litsea* species (except for *L. japonica*) belong in to section *Cylicodaphne*. Clade I contains two *Tomingodaphne* species (*L. pungens* and *L. tsinlingensis*), two *Cylicodaphne* species (*Litsea magnoliifolia* and *Litsea acutivena*), and one *Litsea* species (*L. glutinosa*), while Clade III includes four *Tomingodaphne* taxa (*L. auriculata*, *L. cubeba*, *L. cubeba* var. *formosana*, and *L. mollis*), two *Conodaphne* species (*L. coreana* and *L. monopetala*), and nine *Cylicodaphne* species.

The plastid gene content of land plants does not appear to have changed dramatically, and few gene losses might have taken place during the evolution of land plants (Wicke et al., 2011; Song et al., 2017). Available plastomes of the Lauraceae have similar structures and vary in size from 150 kb to 159 kb, except for genus *Cassytha* (115 kb), which has lost an entire IR region (Song et al., 2017). Throughout the evolution of terrestrial plants, the IR regions have

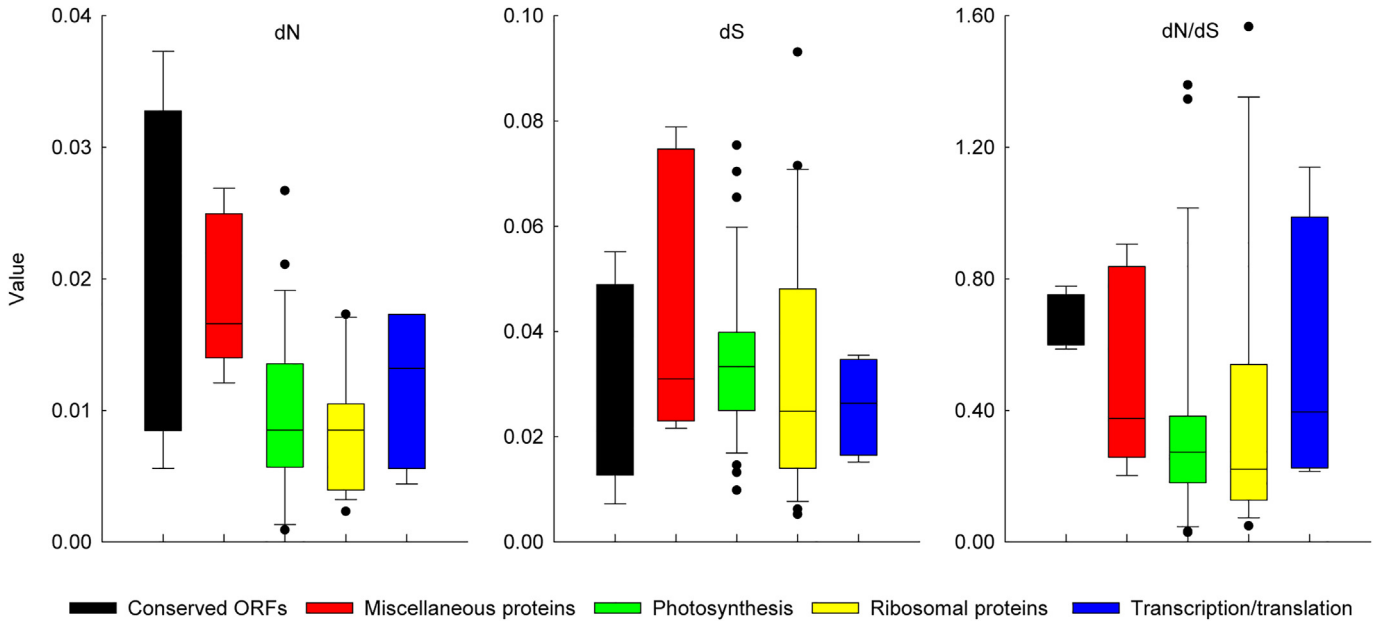

Fig. 7. Positive selection strength of protein-coding genes of the plastomes from 18 taxa.

shown a tendency to expand (Zheng et al., 2020). In this study, we report complete plastome sequences of seven *Litsea* taxa in the tribe Laureae (Lauraceae). The complete plastome size of newly sequenced taxa varies from 152,377 bp (*L. auriculata*) to 154,117 bp (*L. pierrei*). IR region lengths of the 18 taxa of clade III also vary (20,015–21,289 bp) and are shorter than those of *Lagerstroemia* (Zheng et al., 2020) and Monsteroideae (Henriquez et al., 2020). This variation in IR region length differs from that of other species of Lauraceae (Tian et al., 2019; Xiao et al., 2020). In *Litsea* species, variation of plastome size can be largely explained by expansions and contractions of the IR regions. Unlike other Lauraceae plants, the plants of clade III have identical numbers of protein-coding genes (82), transfer RNA genes (tRNA) (36) and ribosome RNA (rRNA) genes (8) (Song et al., 2016, 2017). In contrast to previous studies (Xiao et al., 2020), we found that the plastomes of Lauraceae plants have more *rpl22* and *psbZ* genes than *lhbA* genes.

4.2. Sequence repeats and divergence hotspot analysis

Oligonucleotide repeats play important roles in the generation of substitutions, indels, and inversions (Iram et al., 2019). In this study, analyses of oligonucleotide repeats and SSRs showed similarities among plastomes of the 18 taxa. Most of the repeats ranged between 30 and 34 bp. The most frequent mononucleotide repeats were A/T repeats (97.7%); the remaining 2.3% of mononucleotide repeats were G/C repeats. High proportions of poly A/T have also been reported in previous studies (Zheng et al., 2020; Mehmood et al., 2020; Munyao et al., 2020). Three species (*L. dilleniifolia*, *L. szemaois*, *L. pierrei* var. *szemois*) have a 660-bp indel flanked by poly-A/T repeats.

Divergence hotspots can provide references for the development of accurate, robust, and cost-effective molecular markers for phylogenetic analysis, population genetics and species barcoding (Ahmed et al., 2013). In the 18 plastomes of clade III the regions with the highest nucleotide variability include *trnG-trnR*, *psbM-trnD*, *ycf3-trnS*, *ndhF*, *ndhF-rpl32*, *rpl32-trnL*, *ndhG-ndhI*, and *ycf1*. The highly variable hotspots screened in this study exhibit divergence similar to that of *psbM-trnD*, *ndhF*, and *ycf1* in trinerved *Lindera* species (Tian et al., 2019), and of *ndhF-rpl32*, and *ycf1* in nine *Lindera* species (Zhao et al., 2018). Unlike *Lindera*, the *Litsea* species showed hypervariable regions at the locus of *trnG-trnR*, *ycf3-trnS*, *rpl32-trnL*, and *ndhG-ndhI*. The mini-barcode *ndhF-rpl32* also performed well in distinguishing *Pterocarpus* species (Jiao et al., 2018). The *ndhF*, *ycf1*, and *rpl32* are highly variable in many plants and even used for barcoding (Amar, 2020; Zheng et al., 2020). The highly variable hotspots and polymorphic SSRs in the study may provide references for marker-assisted breeding and identification of *Litsea* cultivars.

4.3. Codon usage and selective pressure analysis

Base composition has a substantial effect on the basic parameters of genome stability and evolution (Kiktev et al., 2018). In the genus *Oryza*, GC content correlates positively with recombination rates, and GC content at the 3′ is positively correlated with expression levels, suggesting that selection favors codons ending with G or C (Muyle et al., 2011). Monocotyledons favor G or C as terminated codons, while dicotyledons favor A or T (Chen et al., 2017). In the current study, *Litsea* GC content is similar to that of *Lindera* species (Xiao et al., 2020), and the codons that end with A or T at the 3′ show high encoding efficacy of the amino acid. The codon usage patterns of *Litsea* species are similar to those reported in *Lagerstroemia* and Monsteroideae, possibly due to the high proportion of A/T in plastomes (Zheng et al., 2020; Henriquez et al., 2020), which illustrates nucleotide composition plays a vital role in the pattern of genes codon usage.

Because recombination events are rare in the plastid genome, it has a low DNA replacement rate and genes are generally conserved (Omelchenko et al., 2020). Our analysis of *Litsea* plastomes shows that 74 of 79 genes have an average of dN/dS < 1, which indicates that, as expected, the evolutionary rate is low in these species. Most of these genes, which are associated with photosynthesis, are crucial and conserved in plants (Liang et al., 2020); thus, no non-synonymous mutations were detected. Six genes (*accD*, *ndhJ*, *rbcL*, *rpoC2*, *ycf1*, and *ycf2*) often associated with photosynthesis and gene transcription possess at least one site under positive selection in *Litsea* (Gao et al., 2019; Wang et al., 2021; Yang et al., 2021). The positive selection of *rbcL* gene, which encodes for the large subunit

of RuBisCO, is fairly common in many land plants (Wen et al., 2021). In *Ilex*, high rates of positive selection on the *rbcL* gene are associated with hybridization and introgression (Yao et al., 2019). The acetyl-CoA carboxylase subunit D gene *accD*, NADH oxidoreductase gene *ndhJ* and the transcription gene *rpoC2* have been shown to be under positive selection pressure in several plant species (Gao et al., 2019; Yang et al., 2021). The functions of *ycf1* and *ycf2* are largely unknown, but they are indispensable for plant cell survival (Drescher et al., 2000). These positively selected genes and nucleotide characteristics found in *Litsea* species may play an important role in helping these plants adapt to various environments.

5. Conclusions

In this study, the plastomes of seven *Litsea* taxa were sequenced for phylogenetic analyses. Our analysis showed that the genus *Litsea* is polyphyletic. Sixteen *Litsea* taxa clustered with two *Lindera* taxa in a monophyletic group. Our findings reveal the phylogenetic relationships of the Laureae species. Comparative analysis of the plastomes of 18 taxa of this monophyletic group revealed a conserved collinear structure and genetic content of the sequences, and provide reliable genetic information for the study of subtribe Lauriineae. We also identified SSR markers and highly variable regions that may serve as significant genetic markers to delimit species/cultivars and provide a reference for marker-assisted breeding. The positive selection of several genes (*accD*, *ndhJ*, *rbcL*, *rpoC2*, *ycf1,* and *ycf2*) may reflect the rapid evolution in some lineages of genus *Litsea*.

Author contributions

YS and CL conceived and designed the work, YHT, LZT and HHC prepared the datasets and discussed the results, CL wrote the manuscript, PKH, LHH and YS revised the manuscript.

Declaration of competing interest

The authors declare no conflict of interest.

Acknowledgments

This research was supported by the National Natural Science Foundation of China (Grant No. 32060710, 31970223, 31860005, 31860620) and Applied Basic Research Projects of Yunnan (Grant No. 2019FB057).

Appendix A. Supplementary data

Supplementary data to this article can be found online at https://doi.org/10.1016/j.pld.2021.11.009.

References

Ahmed, I., Matthews, P.J., Biggs, P.J., et al., 2013. Identification of chloroplast genome loci suitable for high-resolution phylogeographic studies of *Colocasia esculenta* (L.) Schott (Araceae) and closely related taxa. Mol. Ecol. Resour. 13, 929–937. https://doi.org/10.1111/1755-0998.12128.

Amar, M.H., 2020. *ycf1-ndhF* genes, the most promising plastid genomic barcode, sheds light on phylogeny at low taxonomic levels in *Prunus persica*. J. Genet. Eng. Biotechnol. 18, 42. https://doi.org/10.1186/s43141-020-00057-3.

Beier, S., Thiel, T., Münch, T., et al., 2017. MISA-web: a web server for microsatellite prediction. Bioinformatics 33, 2583–2585. https://doi.org/10.1093/bioinformatics/btx198.

Bentham, G., 1880. Laurineae. Genera plantarum 3, 146–168.

Bouckaert, R., Heled, J., Kuhnert, D., et al., 2014. Beast 2: a software platform for Bayesian evolutionary analysis. PLoS Comput. Biol. 10, e1003537. https://doi.org/10.1371/journal.pcbi.1003537.

Chanderbali, A.S., Van Der Werff, H., Renner, S.S., 2001. Phylogeny and historical biogeography of Lauraceae: evidence from the chloroplast and nuclear genomes. Ann. Mo. Bot. Gard. 88, 104–134. https://doi.org/10.2307/2666133.

Chen, C., Chen, H., Zhang, Y., et al., 2020. TBtools - an integrative toolkit developed for interactive analyses of big biological data. Mol. Plant 13, 1194–1202. https://doi.org/10.1016/j.molp.2020.06.009.

Chen, Z., Hu, F., Wang, X., et al., 2017. Analysis of codon usage bias of *Ananas comosus* with genome sequencing data. J. Fruit Sci. 34, 946–955. https://doi.org/10.13925/j.cnki.gsxb.20160375.

Doyle, J.J., Dickson, E.E., 1987. Preservation of plant samples for DNA restriction endonuclease analysis. Taxon 36, 715–722. https://doi.org/10.2307/1221122.

Drescher, A., Ruf, S., Jr, T.C., et al., 2000. The two largest chloroplast genome-encoded open reading frames of higher plants are essential genes. Plant J. 22, 97–104.

Du, X., Zeng, T., Feng, Q., et al., 2020. The complete chloroplast genome sequence of yellow mustard (*Sinapis alba* L.) and its phylogenetic relationship to other Brassicaceae species. Gene 731, 144340. https://doi.org/10.1016/j.gene.2020.144340.

Fijridiyanto, I.A., Murakami, N., 2009a. Molecular systematics of malesian *Litsea* lam. And putative related genera (Lauraceae). Acta Phytotaxon. Geobot. 60, 1–18. https://doi.org/10.18942/apg.KJ00005576218.

Fijridiyanto, I.A., Murakami, N., 2009b. Phylogeny of *Litsea* and related genera (Laureae-Lauraceae) based on analysis of *rpb2* gene sequences. J. Plant Res. 122, 283–298. https://doi.org/10.1007/s10265-009-0218-8.

Gao, L.Z., Liu, Y.L., Zhang, D., et al., 2019. Evolution of *Oryza* chloroplast genomes promoted adaptation to diverse ecological habitats. Commun. Biol. 2, 278. https://doi.org/10.1038/s42003-019-0531-2.

Greiner, S., Lehwark, P., Bock, R., 2019. OrganellarGenomeDRAW (OGDRAW) version 1.3.1: expanded toolkit for the graphical visualization of organellar genomes. Nucleic Acids Res. 47, W59–W64. https://doi.org/10.1093/nar/gkz238.

Henriquez, C.L., Abdullah, Ahmed, I., et al., 2020. Molecular evolution of chloroplast genomes in Monsteroideae (Araceae). Planta 251, 72. https://doi.org/10.1007/s00425-020-03365-7.

Hinsinger, D.D., Strijk, J.S., 2017. Toward phylogenomics of Lauraceae: the complete chloroplast genome sequence of *Litsea glutinosa* (Lauraceae), an invasive tree species on Indian and Pacific Ocean islands. Plant Gene 9, 71–79. https://doi.org/10.1016/j.plgene.2016.08.002.

Iram, S., Hayat, M.Q., Tahir, M., et al., 2019. Chloroplast genome sequence of *Artemisia scoparia*: comparative analyses and screening of mutational hotspots. Plants 8, 476. https://doi.org/10.3390/plants8110476.

Jiao, L., Yu, M., Wiedenhoeft, A.C., et al., 2018. DNA barcode authentication and library development for the wood of six commercial *Pterocarpus* species: the critical role of xylarium specimens. Sci. Rep. 8, 1945. https://doi.org/10.1038/s41598-018-20381-6.

Jin, J.J., Yu, W.B., Yang, J.B., et al., 2020. GetOrganelle: a fast and versatile toolkit for accurate de novo assembly of organelle genomes. Genome Biol. 21, 241. https://doi.org/10.1186/s13059-020-02154-5.

Jo, S., Kim, Y.K., Cheon, S.H., et al., 2019. Characterization of 20 complete plastomes from the tribe Laureae (Lauraceae) and distribution of small inversions. PLoS One 14, e0224622. https://doi.org/10.1371/journal.pone.0224622.

Kamle, M., Mahato, D.K., Lee, K.E., et al., 2019. Ethnopharmacological properties and medicinal uses of *Litsea cubeba*. Plants 8, 150. https://doi.org/10.3390/plants8060150.

Katoh, K., Rozewicki, J., Yamada, K.D., 2019. MAFFT online service: multiple sequence alignment, interactive sequence choice and visualization. Briefings Bioinf. 20, 1160–1166. https://doi.org/10.1093/bib/bbx108.

Kearse, M., Moir, R., Wilson, A., et al., 2012. Geneious Basic: an integrated and extendable desktop software platform for the organization and analysis of sequence data. Bioinformatics 28, 1647–1649. https://doi.org/10.1093/bioinformatics/bts199.

Kiktev, D.A., Sheng, Z., Lobachev, K.S., et al., 2018. GC content elevates mutation and recombination rates in the yeast *Saccharomyces cerevisiae*. Proc. Natl. Acad. Sci. U.S.A. 115, E7109–E7118. https://doi.org/10.1073/pnas.1807334115.

Kumar, S., Stecher, G., Li, M., et al., 2018. Mega X: molecular evolutionary genetics analysis across computing platforms. Mol. Biol. Evol. 35, 1547–1549. https://doi.org/10.1093/molbev/msy096.

Kurtz, S., Choudhuri, J.V., Ohlebusch, E., et al., 2001. REPuter: the manifold applications of repeat analysis on a genomic scale. Nucleic Acids Res. 29, 4633–4642. https://doi.org/10.1093/nar/29.22.4633.

Li, J., Christophel, D.C., 2000. Systematic relationships within the *Litsea* complex (Lauraceae): a cladistic analysis on the basis of morphological and leaf cuticle data. Aust. Syst. Bot. 13, 1–13. https://doi.org/10.1071/SB98015.

Li, J., Christophel, D.C., Conran, J.G., et al., 2004. Phylogenetic relationships within the 'core' Laureae (*Litsea* complex, Lauraceae) inferred from sequences of the chloroplast gene *matK* and nuclear ribosomal DNA ITS regions. Plant Syst. Evol. 246, 19–34. https://doi.org/10.1007/s00606-003-0113-z.

Li, J., Conran, J.G., Christophel, D.C., et al., 2008. Phylogenetic relationships of the *Litsea* complex and core Laureae (Lauraceae) using ITS and ETS sequences and morphology. Ann. Mo. Bot. Gard. 95, 580–599. https://doi.org/10.3417/2006125.9504.

Liang, H., Zhang, Y., Deng, J., et al., 2020. The complete chloroplast genome sequences of 14 *Curcuma* species: insights into genome evolution and phylogenetic relationships within Zingiberales. Front. Genet. 11, 802. https://doi.org/10.3389/fgene.2020.00802.

Liu, C., Chen, H., Han, L., et al., 2020. The complete plastid genome of an evergreen tree *Litsea elongata* (Lauraceae: Laureae). Mitochondrial DNA B 5, 2483–2484. https://doi.org/10.1080/23802359.2020.1778566.

Mehmood, F., Abdullah, Shahzadi, I., et al., 2020. Characterization of *Withania somnifera* chloroplast genome and its comparison with other selected species of Solanaceae. Genomics 112, 1522–1530. https://doi.org/10.1016/j.ygeno.2019.08.024.
Minh, B.Q., Schmidt, H.A., Chernomor, O., et al., 2020. IQ-TREE 2: new models and efficient methods for phylogenetic inference in the genomic era. Mol. Biol. Evol. 37, 1530–1534. https://doi.org/10.1093/molbev/msaa015.
Munyao, J.N., Dong, X., Yang, J.X., et al., 2020. Complete chloroplast genomes of *Chlorophytum comosum* and *Chlorophytum gallabatense*: genome structures, comparative and phylogenetic analysis. Plants 9, 296. https://doi.org/10.3390/plants9030296.
Muyle, A., Serres-Giardi, L., Ressayre, A., et al., 2011. GC-biased gene conversion and selection affect GC content in the *Oryza* genus (rice). Mol. Biol. Evol. 28, 2695–2706. https://doi.org/10.1093/molbev/msr104.
Omelchenko, D.O., Krinitsina, A.A., Belenikin, M.S., et al., 2020. Complete plastome sequencing of *Allium paradoxum* reveals unusual rearrangements and the loss of the ndh genes as compared to *Allium ursinum* and other onions. Gene 726, 144154. https://doi.org/10.1016/j.gene.2019.144154.
Rozas, J., Ferrer-Mata, A., Sánchez-Delbarrio, J.C., et al., 2017. DnaSP 6: DNA sequence polymorphism analysis of large data sets. Mol. Biol. Evol. 34, 3299–3302. https://doi.org/10.1093/molbev/msx248.
Song, Y., Yao, X., Tan, Y., et al., 2016. Complete chloroplast genome sequence of the avocado: gene organization, comparative analysis, and phylogenetic relationships with other Lauraceae. Can. J. For. Res. 46, 1293–1301. https://doi.org/10.1139/cjfr-2016-0199.
Song, Y., Yu, W.B., Tan, Y., et al., 2017. Evolutionary comparisons of the chloroplast genome in Lauraceae and insights into loss events in the Magnoliids. Genome Biol. Evol. 9, 2354–2364. https://doi.org/10.1093/gbe/evx180.
Song, Y., Yu, W.B., Tan, Y.H., et al., 2020. Plastid phylogenomics improve phylogenetic resolution in the Lauraceae. J. Syst. Evol. 58, 423–439. https://doi.org/10.1111/jse.12536.
Tian, X., Ye, J., Song, Y., 2019. Plastome sequences help to improve the systematic position of trinerved *Lindera* species in the family Lauraceae. PeerJ 7, e7662. https://doi.org/10.7717/peerj.7662.
Wang, J.H., Moore, M.J., Wang, H., et al., 2021. Plastome evolution and phylogenetic relationships among Malvaceae subfamilies. Gene 765. https://doi.org/10.1016/j.gene.2020.145103.
Wang, Y.S., Wen, Z.Q., Li, B.T., et al., 2016. Ethnobotany, phytochemistry, and pharmacology of the genus *Litsea*: an update. J. Ethnopharmacol. 181, 66–107. https://doi.org/10.1016/j.jep.2016.01.032.
Wen, F., Wu, X., Li, T., et al., 2021. The complete chloroplast genome of *Stauntonia chinensis* and compared analysis revealed adaptive evolution of subfamily Lardizabaloideae species in China. BMC Genom. 22, 161. https://doi.org/10.1186/s12864-021-07484-7.
Wicke, S., Schneeweiss, G.M., Depamphilis, C.W., et al., 2011. The evolution of the plastid chromosome in land plants: gene content, gene order, gene function. Plant Mol. Biol. 76, 273–297. https://doi.org/10.1007/s11103-011-9762-4.
Xiao, T., Xu, Y., Jin, L., et al., 2020. Conflicting phylogenetic signals in plastomes of the tribe Laureae (Lauraceae). PeerJ 8, e10155. https://doi.org/10.7717/peerj.10155.
Xu, B., Yang, Z., 2013. PAMLX: a graphical user interface for PAML. Mol. Biol. Evol. 30, 2723–2724. https://doi.org/10.1093/molbev/mst179.
Yadav, G., Goswami, B., 1990. Studies on the foliar constituents of food plants of muga silkworm (*Antheraea assama* Westwood). J. Ecobiol. 2, 222–228.
Yang, J., Chiang, Y.C., Hsu, T.W., et al., 2021. Characterization and comparative analysis among plastome sequences of eight endemic *Rubus* (Rosaceae) species in Taiwan. Sci. Rep. 11, 1152. https://doi.org/10.1038/s41598-020-80143-1.
Yao, X., Tan, Y.H., Yang, J.B., et al., 2019. Exceptionally high rates of positive selection on the *rbcL* gene in the genus *Ilex* (Aquifoliaceae). BMC Evol. Biol. 19, 192. https://doi.org/10.1186/s12862-019-1521-1.
Zhang, Y., Tian, Y., Tng, D.Y.P., et al., 2021. Comparative chloroplast genomics of *Litsea* Lam. (Lauraceae) and its phylogenetic implications. Forests 12, 744. https://doi.org/10.3390/f12060744.
Zhang, T., Zeng, C.X., Yang, J.B., et al., 2016. Fifteen novel universal primer pairs for sequencing whole chloroplast genomes and a primer pair for nuclear ribosomal DNAs. J. Syst. Evol. 54, 219–227. https://doi.org/10.1111/jse.12197.
Zhao, M.L., Song, Y., Ni, J., et al., 2018. Comparative chloroplast genomics and phylogenetics of nine *Lindera* species (Lauraceae). Sci. Rep. 8, 8844. https://doi.org/10.1038/s41598-018-27090-0.
Zheng, G., Wei, L., Ma, L., et al., 2020. Comparative analyses of chloroplast genomes from 13 *Lagerstroemia* (Lythraceae) species: identification of highly divergent regions and inference of phylogenetic relationships. Plant Mol. Biol. 102, 659–676. https://doi.org/10.1007/s11103-020-00972-6.